Gamma radiation effects on silicon photonic waveguides

STEFANO GRILLANDA,[1,*] VIVEK SINGH,[2,A] VIVEK RAGHUNATHAN,[2,B] FRANCESCO MORICHETTI,[1] ANDREA MELLONI,[1] LIONEL KIMERLING,[2] AND ANURADHA M. AGARWAL[3]

[1]*Politecnico di Milano, Dipartimento di Elettronica, Informazione e Bioingegneria, 20133 Milano, Italy*
[2]*Massachusetts Institute of Technology, Department of Materials Science and Engineering, Cambridge, Massachusetts 02139, USA*
[3]*Massachusetts Institute of Technology, Materials Processing Center, Cambridge, Massachusetts 02139, USA*
[A]*Now with Saint Gobain*
[B]*Now with Intel Corp.*
**Corresponding author: stefano.grillanda@polimi.it*

Received XX Month XXXX; revised XX Month, XXXX; accepted XX Month XXXX; posted XX Month XXXX (Doc. ID XXXXX); published XX Month XXXX

To support the use of integrated photonics in harsh environments, such as outer space, their hardness threshold to high-energy radiation must be established. Here, we investigate the effects of gamma (γ) rays, with energy in the MeV-range, on silicon photonic waveguides. By irradiation of high-quality factor amorphous silicon core resonators we measure the impact of γ-rays on the materials incorporated in our waveguide system, namely amorphous silicon, silicon dioxide and polymer. While we show the robustness of amorphous silicon and silicon dioxide up to an absorbed dose of 15 Mrad, more than 100x higher than previous reports on crystalline silicon, polymer materials exhibit changes with doses as low as 1 Mrad.

OCIS codes: *(130.0130) Integrated Optics; (230.5750) Resonators; (230.7370) Waveguides; (350.5610) Radiation.*

http://dx.doi.org/10.1364/OL.99.099999

Photonic integrated technologies are currently under consideration by the major space agencies for use in future space systems including satellites, space-crafts and space stations [1-3]. In fact, integrated optical circuits have the potential to increase the capacity and reduce cost, volume and weight of today's space communication systems based on microwave and electronic components. However, space is a harsh environment, where devices are constantly exposed to a multitude of sources of high-energy radiation, which can have a strong impact on their long-term behavior [4]. For this reason, before deployment of photonics in space, it is essential to investigate the effects of high-energy irradiation on optical devices and materials to identify their radiation sensitivity and hardness. The physical mechanisms responsible for damage in the materials in space are equally applicable to other harsh environments, such as near nuclear reactors or high-energy particle colliders [4].

Although in the last decades many works have investigated the impact of high-energy radiation on electronic devices [5], optoelectronic materials [6-7] and fiber optic components [8], only very few have addressed radiation effects on photonic integrated circuits [9-12]. Microring resonators (MRRs) fabricated in crystalline silicon (Si) have been exposed to ionizing *x*-rays and γ-rays [9], with corresponding energies of 10 keV and 662 keV. While passivated MRRs exhibit a radiation-hard behavior up to 145 krad and 147 krad, respectively for *x*- and γ-irradiation, the resonance of unpassivated resonators exhibit a blue-shift, which was attributed to an accelerated oxidation of the Si surface induced by the irradiation. Si Mach-Zehnder interferometers, with heavily doped regions to achieve fast modulation, were exposed to neutrons and *x*-rays [10], with corresponding energies of 20 MeV (total fluence $1.2 \cdot 10^{15}$ neutrons/cm^2) and 10 keV (total dose 130 Mrad). A degradation of the modulation efficiency was observed after *x*-ray exposure, which was attributed to the creation of interface traps in the oxide layers of the waveguide, which in turn

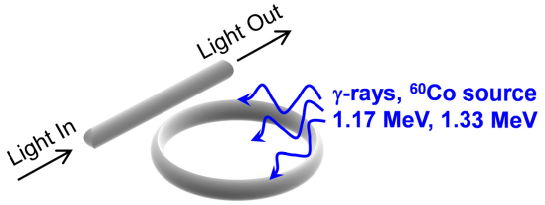

Fig. 1. a-Si microring resonators have been exposed to γ-radiation by using a ^{60}Co source emitting two cascade γ-rays with energies of 1.17 MeV and 1.33 MeV. A total absorbed dose of 15 Mrad has been achieved.

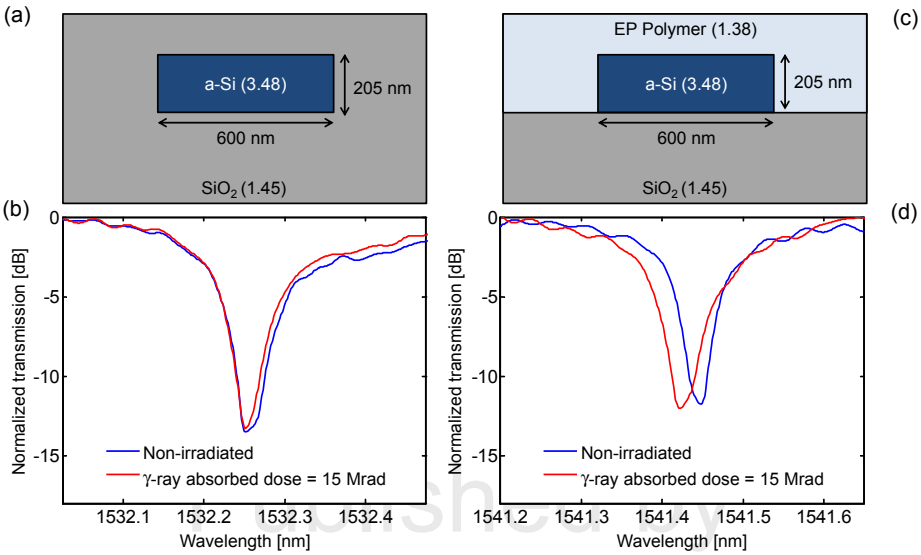

Fig. 2. Schematic of the cross-section of the a-Si waveguides considered in this work: (a) one coated with SiO_2, (c) the other with EP polymer. **Comparison of the TM-polarized transfer function of microring resonators coated with (b) SiO_2 and (d) EP polymer before (blue) and after (red) exposure to γ-rays.** The **measured** variations in the microring resonance and linewidth can be associated with the polymer, whereas a-Si and SiO_2 exhibit a radiation-hard behavior up to 15 Mrad.

affects the location of the free carriers in the Si core and thus the modulation performance. Silicon nitride MRRs were exposed to proton irradiation with energies in the range between 18.3 MeV and 99.7 MeV [11]: no appreciable effect was observed up to a fluence of $1.516 \cdot 10^{10}$ protons/cm^2. Lithium niobate waveguides were found to experience larger propagation loss after exposure to γ-radiation up to a dose of 10 Mrad (energies of 1.17 MeV and 1.33 MeV) [12].

In this Letter, we investigate the effects of high-energy γ-radiation on amorphous Si (a-Si) photonic waveguides. Two waveguide structures are investigated, one coated with silicon dioxide (SiO_2), the other with polymer to realize athermal devices, the latter being very appealing for space environments where extreme temperature variations typically occur. With respect to other reports **about crystalline Si waveguides** [9], in addition to using an amorphous Si technology, we increase the total irradiation dose experienced by the Si waveguides (up to 15 Mrad) by more than 100 times, and exploit a different γ-radiation source enabling higher energy exposure (in the MeV-energy-range).

The effects of γ-radiation on a-Si photonic waveguides were investigated through an extensive characterization of high quality factor MRRs in all-pass filter configuration (Fig. 1). From the measured changes in the MRRs resonance and linewidth we were able to find the impact of radiations on the materials that constitute our waveguides. Exposure to radiation was performed with a Cobalt-60 (^{60}Co) source, available at Massachusetts Institute of Technology, which emits two cascade γ-rays with energies of 1.17 MeV and 1.33 MeV. All the samples considered in this work were entirely and uniformly exposed to the radiation.

Figure 2(a) shows a cross-sectional view of the Si waveguides that were irradiated in this work. A 205 nm thick layer of a-Si was deposited on a Si wafer with a 3 µm thick SiO_2 thermal oxide, using plasma enhanced chemical vapor deposition at 200°C using silane (SiH4, 60 sccm) and argon (Ar, 300 sccm). Additional details on the a-Si deposition conditions can be found in [13]. **Channel waveguides with 600 nm width were patterned by means of photolithography using an i-line stepper.** On top of it a 3 µm thick oxide is deposited by means of chemical vapor deposition.

The blue line in Fig. 2(b) shows the normalized transmission of the non-irradiated MRR measured on transverse magnetic polarization (TM). Spectral measurements are performed using an optical vector analyzer. Light is coupled at the input and output of the chip by means of lensed fibers with 1.7 µm mode-field-diameter. The temperature of the chip is controlled using a thermo-electric cooler with a temperature stability of better than ±0.1°C. The resonator has a racetrack layout, with length of 426 µm and measured free-spectral-range of 1.86 nm (237.1 GHz) on TM polarization. The microring has an on-resonance extinction ratio of almost 14 dB, a -3 dB linewidth of about 154 pm (19.7 GHz) and a quality factor of $9.9 \cdot 10^3$.

The MRR transmission was then measured after exposure to γ-radiation. Several irradiation cycles were performed, achieving a total absorbed dose of γ-rays of 15 Mrad. Due to the very high-energy and high-doses involved in the irradiation experiments, the chip was kept sealed in the γ-ray source machine during the exposure cycles. Therefore the MRR transmission was not measured in real time during the irradiation, but instead was measured after every exposure, and compared to the non-irradiated curve [blue line in Fig. 2(b)]. This means that lasting effects induced by the high-energy irradiation are studied here, as opposed to temporary or transient effects.

The red line in Fig. 2(b) shows the normalized transmission of the MRR after 15 Mrad γ-ray exposure. No appreciable wavelength shift of the microring resonance is measured, thus suggesting that no significant variation of the effective index is experienced by the waveguides. Also, no significant change in the linewidth or in the extinction ratio is observed, thus indicating that the quality factor of the MRR remains the same after irradiation. This means that no change in the refractive index, propagation loss or backscattering level is experienced by these waveguides after exposure to 15 Mrad of γ-rays. Given the deep penetration of γ-radiation across the materials stack of Fig. 2(a) and the **lower confinement factor of**

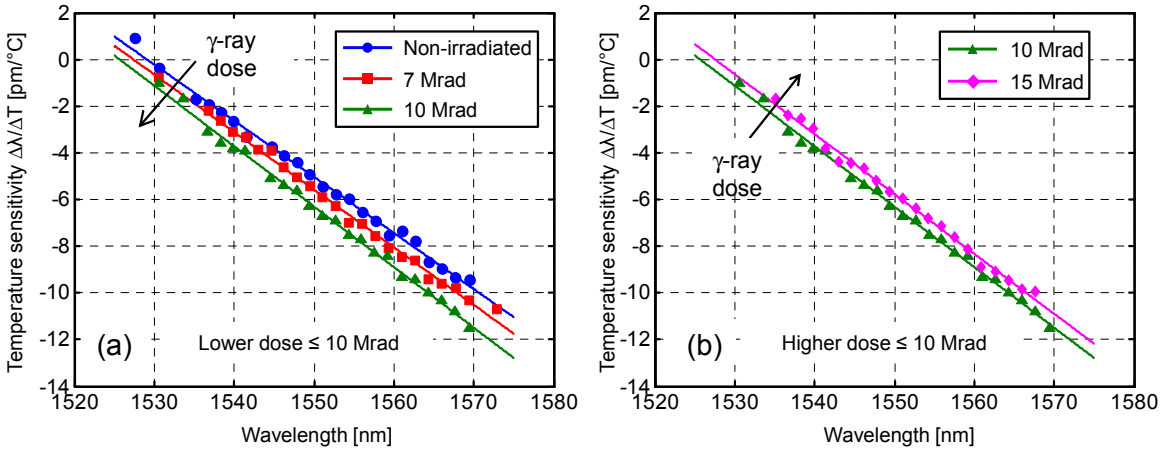

Fig. 3. Temperature sensitivity $\Delta\lambda/\Delta T$ as a function of wavelength of the microring resonators coated with polymer for different absorbed doses of γ-radiation up to 15 Mrad: (a) a blue-shift of the $\Delta\lambda/\Delta T$ curve and of the athermal wavelength is observed for lower doses (≤10 Mrad); (b) a red-shift is measured for higher doses (≥ 10 Mrad).

the TM mode in the Si core (about 35%) with respect to the TE mode, the observed radiation-hard behavior of these waveguides indicates that both materials (a-Si and SiO_2) are robust against this irradiation. This result extends the radiation-hard behavior of silicon to more than 100x with respect to previous reports [9].

Figures 2(c-d) show the results of the γ-irradiation experiments performed on polymer coated a-Si waveguides. The waveguide geometry and materials are the same as in the previous experiment [Figs. 2(a-b)], except for the 3 μm thick top cladding that is a hyperlinked fluoropolymer, proprietary of Enablence Inc., and named EP [14]. After spin-coating the polymer cladding on top of the waveguides, the samples were exposed to ultraviolet light (with an intensity of 5 mW/cm^2 for 20 min) and baked in vacuum (at 150°C for 4h) to cure and stabilize the polymer properties [14].

As shown in Fig. 3, the waveguide design of Fig. 2(c) is made to achieve full athermal operation at a given wavelength and reduced temperature sensitivity across a large wavelength range with respect to the SiO_2-coated non-athermal waveguides. The design rule of this waveguide is based on the sharing of the optical mode between the core and the top cladding. In fact about 27% of the fundamental TM mode is confined in the polymer upper cladding. As the polymer has a negative thermo-optic coefficient ($-2.65\cdot10^{-4}$ 1/°C), opposite to that of the a-Si core ($2.3\cdot10^{-4}$ 1/°C), this design enables athermal operation. Additional details on the design and performance of these waveguides can be found in [15].

Figure 2(d) shows the results of the irradiation experiments performed on this waveguide technology. As in the case of Fig. 2(c) a total absorbed dose of γ-radiation of 15 Mrad was achieved. The transmission of the MRR before the irradiation is represented by blue line in Fig. 2(d). The ring length is 426 μm, achieving a free-spectral-range of 1.582 nm (199.5 GHz). The -3 dB linewidth of the MRR is 94 pm (11.9 GHz), with a quality factor of $1.6\cdot10^4$ and an extinction ratio of about 12 dB.

After irradiation the microring resonant wavelength blue-shifts by about 21 pm (3.4 GHz), a behavior that is consistent with a variation of the effective index of the waveguide of about $-4.8\cdot10^{-5}$. Based on the results of Figs. 2(a-b) obtained on the SiO_2-coated waveguides, this resonance shift can be attributed only to a change in the refractive index of the polymer top cladding, whereas those of the a-Si and SiO_2 materials remain the same after exposure. Also, after γ-irradiation the linewidth of the MRR increases to 124 pm (15.7 GHz), resulting in a 33% reduction of the resonator quality factor, that amounts to $1.2\cdot10^4$ after exposure. As the free-spectral-range of the microring is reduced by only 0.3 GHz after irradiation (that is about 0.1%), the corresponding increase in the waveguide group index ($5.3\cdot10^{-3}$) does not explain the larger linewidth, which on the contrary can be attributed only to a variation of the waveguide propagation loss or to the ring coupling coefficient.

We now evaluate the effects of the high-energy γ-radiation on the athermal functionality of these waveguides. Figures 3(a-b) show the measured temperature sensitivity $\Delta\lambda/\Delta T$ as a function of wavelength for the waveguides of Fig. 2(c) in the temperature range 30°C-50°C and for different irradiation doses up to 15 Mrad. The $\Delta\lambda/\Delta T$ curve is obtained from the measurement of the MRR resonant wavelength shift induced by the temperature variations. **Markers indicate the experimental points and solid lines the linear fit of the measured data. Blue line and circle markers in Fig. 3(a) show the temperature sensitivity of the non-irradiated microring from 1525 nm to 1575 nm.** At a wavelength of about 1529 nm no appreciable temperature dependence is experienced by these waveguides. This wavelength is hereinafter named athermal point. Further, the $\Delta\lambda/\Delta T$ curve varies from about 1 pm/°C to **-10 pm/°C** across the 50 nm wavelength range, a sensitivity that is more than 10x smaller than the typical temperature dependence of non-athermal Si waveguides [15].

Figure 3(a) also reports the $\Delta\lambda/\Delta T$ curves measured for higher absorbed irradiation doses up to 10 Mrad (green line and triangle markers). While the dose of absorbed γ-radiation increases, the temperature sensitivity curve of the microrings monotonically blue-shifts in wavelength, in such a way that after a 10 Mrad dose the athermal point of the waveguides is blue-shifted by more than 4 nm, with the slope of the $\Delta\lambda/\Delta T$ curve remaining about the same. Actually, when the radiation dose is further increased to more than 10 Mrad [Fig. 3(b)] the measured behavior is opposite: any additional increase of the dose corresponds to a red-shift of the temperature dependence curve. **No additional increase in the spread of the experimental points of Fig. 3 is observed when increasing the irradiation dose.**

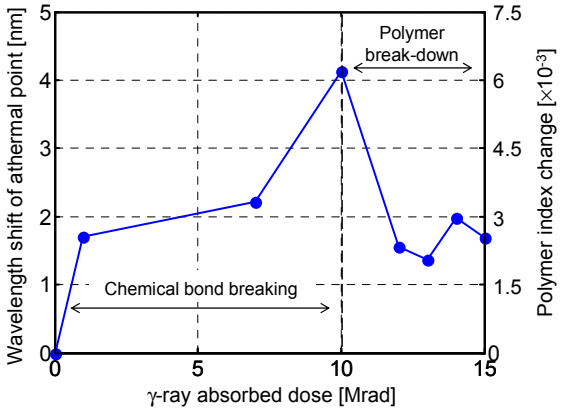

Fig. 4. Absolute value of wavelength shift experienced by the athermal point of the temperature sensitivity curve of Fig. 3 for different doses of γ-rays. The rightmost axis indicates the corresponding change in the polymer index. Smaller doses (<10 Mrad) induce polymer bond breaking, resulting in an index increase; higher doses (>10 Mrad) induce structural degradation leading to an index decrease.

Figure 4 **shows** a plot of the absolute value of the wavelength shift experienced by the athermal point of the $\Delta\lambda/\Delta T$ curve as a function of the absorbed dose of γ-radiation. **This plot** can be used to explain the blue-shift followed by the red-shift **of the $\Delta\lambda/\Delta T$ curve shown** in Fig. 3. After the initial blue-shift experienced for the lower irradiation doses (<10 Mrad), the athermal point is red-shifted toward its initial value for the higher irradiation doses (>10 Mrad). At the end of the γ-radiation exposure (total absorbed dose is 15 Mrad) the position of the athermal point is red-shifted by almost 2 nm with respect to the non-irradiated condition. Figure 4 also shows on its right-most vertical axis the corresponding refractive index change experienced by the polymer during the irradiation **(reported values refer to the index variation with respect to the non-irradiated case at the athermal wavelength).** This is obtained from electromagnetic simulations performed **with the** film mode matching method. The observed behavior is compatible with an initial increase of the refractive index of the polymer, amounting to a variation of about $6.2\cdot10^{-3}$ for an absorbed dose of 10 Mrad. Then, higher doses of γ-irradiation are responsible for a reduction of the polymer index, inducing a total variation of $2.5\cdot10^{-3}$ for an absorbed dose of 15 Mrad.

This behavior experienced by the refractive index of the polymer is in line to that typical of polymers under exposure to high-energy radiation [16]. In fact, polymers may exhibit changes in structure without requiring high radiation doses [17]. Crosslinking is promoted in non-crosslinked polymers, but radiation is responsible for degradation of molecular weight (due to chain scission and free radical formation) in crosslinked polymers. Increasing the number of broken bonds will also increase the polarizability of the polymer, thus leading to a refractive index increase. As the polymer that we use is a heavily crosslinked fluoropolymer, the measured increase in its effective index for doses up to 10 Mrad is caused either by an increase in the amount of crosslinking or by the breaking of the chemical bonds in the polymer. At higher doses the rise in the effective index saturates, and additional exposure (>10 Mrad) leads to an index decrease due to a structural degradation of the polymer.

In conclusion, we experimentally investigated the effects of high-energy (1.17, 1.33 MeV) and high-dose (up to 15 Mrad) γ-radiation on Si photonic waveguides. Through the exposure and measurement of high-quality factor resonators we were able to establish the hardness and sensitivity levels to γ-rays of the materials incorporated in our waveguide technologies, namely a-Si, SiO_2 and EP polymer. Neither resonance shifts nor linewidth variations were observed on a-Si microrings coated with SiO_2 up to a total absorbed dose of 15 Mrad, thus **demonstrating** the radiation-hard behavior of a-Si and SiO_2 materials to γ-rays up to this radiation level, more than 100x higher than other reports related to Si photonics [9]. On the contrary, a-Si resonators coated with EP polymer to realize athermal devices exhibited both resonant wavelength shifts (21 pm blue-shift at 15 Mrad) and quality factor variations (33% reduction at 15 Mrad), which were attributed to changes occurring in the polymer under γ-radiation.

Funding. This work was funded by the Defense Threat Reduction Agency Grant No. HDTRA1-13-1-0001 and Progetto Rocca Foundation.

Acknowledgment. The authors thank T. Izuhara for support with the polymer spin-coating.

References

1. D. Cornwell, Optics & Photonics News **27**, 24 (2016).
2. NASA (2016), "NASA engineers tapped to build first integrated-photonics modem," http://www.nasa.gov/feature/goddard/2016/nasa-engineers-tapped-to-build-first-integrated-photonics-modem.
3. N. Karafolas, J. M. P. Armengol, and I. Mckenzie, *IEEE Aerospace conference 2009*, p.15.
4. A. H. Johnston, IEEE Trans. Nucl. Sci. **60**, 2054 (2013).
5. R. Schwank, V. Ferlet-Cavrois, M. R. Shaneyfelt, P. Paillet, and P. E. Dodd, IEEE Trans. Nucl. Sci. **50**, 522 (2003).
6. E. Colby, G. Lum, T. Plettner, and J. Spencer, IEEE Trans. Nucl. Sci. **49**, 2857 (2002).
7. N. S. Patel, C. Monmeyran, A. Agarwal, and L. C. Kimerling, J. Appl. Phys. **118**, 155702 (2015).
8. A. I. Gusarov, F. Berghmans, O. Deparis, A. Fernandez Fernandez, Y. Defosse, P. Mégret, M. Décreton, and M. Blondel, IEEE Photon. Technol. Lett. **11**, 1159 (1999).
9. S. Bhandaru, S. Hu, D. M. Fleetwood, and S. M. Weiss, IEEE Trans. Nucl. Sci **62**, 323 (2015).
10. S. Storey, F. Boeuf, C. Baudot, S. Detraz, J. M. Fedeli, D. Marris-Morini, L. Olantera, G. Pezzullo, C. Sigaud, C. Soos, J. Troska, F. Vasey, L. Vivien, M. Zeiler, and M. Ziebell, IEEE Trans. Nucl. Sci. **62**, 329 (2015).
11. V. Brasch, Q.-F. Chen, S. Schiller, and T. J. Kippenberg, Opt. Exp. **22**, 30786 (2014).
12. C.-C. Lai, C.-Y. Chang, Y.-Y. Wei, and W.-S. Wang, IEEE Photon. Technol. Lett. **19**, 1002 (2007).
13. D. K. Sparacin, R. Sun, A. M. Agarwal, M. A. Beals, J. Michel, L. C. Kimerling, T. J. Conway, A. T. Pomerene, D. N. Carothers, M. J. Grove, D. M. Gill, M. S. Rasras, S. S. Patel, and A. E. White, in *3rd IEEE International Conference on Group IV Photonics* (IEEE, 2006), pp. 255–257.
14. V. Raghunathan, T. Izuhara, J. Michel, and L. Kimerling, Opt. Exp. **20**, 16059 (2012).
15. V. Raghunathan, W. N. Ye, J. Hu, T. Izuhara, J. Michel, and L. Kimerling, Opt. Exp. **18**, 17631 (2010).
16. C.-C. Lai, T.-Y. Wei, C.-Y. Chang, W.-S. Wang, and Y.-Y. Wei, Appl. Phys. Lett. **92**, 023303 (2008).
17. N. Borodinov, J. Giammarco, N. Patel, A. Agarwal, K. R. O'Donnell, C. J. Kucera, L. G. Jacobsohn, and I. Luzinov, ACS Appl. Mater. Interfaces **7**, 19455 (2015).

References

1. D. Cornwell, "Space-Based Laser Communications Break Threshold," Optics & Photonics News **27**, 24 (2016).
2. NASA (2016), "NASA engineers tapped to build first integrated-photonics modem," http://www.nasa.gov/feature/goddard/2016/nasa-engineers-tapped-to-build-first-integrated-photonics-modem.
3. N. Karafolas, J. M. P. Armengol, and I. Mckenzie, "Introducing photonics in spacecraft engineering: ESA's strategic approach," *IEEE Aerospace conference 2009*, p.15.
4. A. H. Johnston, "Radiation effects in optoelectronic devices," IEEE Trans. Nucl. Sci. **60**, 2054 (2013).
5. R. Schwank, V. Ferlet-Cavrois, M. R. Shaneyfelt, P. Paillet, and P. E. Dodd, "Radiation Effects in SOI Technologies," IEEE Trans. Nucl. Sci. **50**, 522 (2003).
6. E. Colby, G. Lum, T. Plettner, and J. Spencer, "Gamma radiation studies on optical materials," IEEE Trans. Nucl. Sci. **49**, 2857 (2002).
7. N. S. Patel, C. Monmeyran, A. Agarwal, and L. C. Kimerling, "Point defect states in Sb-doped germanium," J. Appl. Phys. **118**, 155702 (2015).
8. A. I. Gusarov, F. Berghmans, O. Deparis, A. Fernandez Fernandez, Y. Defosse, P. Mégret, M. Décreton, and M. Blondel, "High total dose radiation effects on temperature sensing fiber Bragg gratings," IEEE Photon. Technol. Lett. **11**, 1159 (1999).
9. S. Bhandaru, S. Hu, D. M. Fleetwood, and S. M. Weiss, "Total ionizing dose effects on silicon ring resonators," IEEE Trans. Nucl. Sci **62**, 323 (2015).
10. S. Storey, F. Boeuf, C. Baudot, S. Detraz, J. M. Fedeli, D. Marris-Morini, L. Olantera, G. Pezzullo, C. Sigaud, C. Soos, J. Troska, F. Vasey, L. Vivien, M. Zeiler, and M. Ziebell, "Effect of radiation on a Mach-Zehnder interferometer silicon modulator for HL-LHC data transmission applications," IEEE Trans. Nucl. Sci. **62**, 329 (2015).
11. V. Brasch, Q.-F. Chen, S. Schiller, and T. J. Kippenberg, "Radiation hardness of high-Q silicon nitride microresonators for space compatible integrated optics," Opt. Exp. **22**, 30786 (2014).
12. C.-C. Lai, C.-Y. Chang, Y.-Y. Wei, and W.-S. Wang, "Study of gamma-irradiation damage in LiNbO3 waveguides," IEEE Photon. Technol. Lett. **19**, 1002 (2007).
13. D. K. Sparacin, R. Sun, A. M. Agarwal, M. A. Beals, J. Michel, L. C. Kimerling, T. J. Conway, A. T. Pomerene, D. N. Carothers, M. J. Grove, D. M. Gill, M. S. Rasras, S. S. Patel, and A. E. White, "Low loss amorphous silicon channel waveguides for integrated photonics," in *3rd IEEE International Conference on Group IV Photonics* (IEEE, 2006), pp. 255–257.
14. V. Raghunathan, T. Izuhara, J. Michel, and L. Kimerling, "Stability of polymer-dielectric bi-layers for athermal silicon photonics," Opt. Exp. **20**, 16059 (2012).
15. V. Raghunathan, W. N. Ye, J. Hu, T. Izuhara, J. Michel, and L. Kimerling, "Athermal operation of silicon waveguides: spectral, second order and footprint dependencies," Opt. Exp. **18**, 17631 (2010).
16. C.-C. Lai, T.-Y. Wei, C.-Y. Chang, W.-S. Wang, and Y.-Y. Wei, "Gamma-ray irradiated polymer optical waveguides," Appl. Phys. Lett. **92**, 023303 (2008).
17. N. Borodinov, J. Giammarco, N. Patel, A. Agarwal, K. R. O'Donnell, C. J. Kucera, L. G. Jacobsohn, and I. Luzinov, "Stability of grafted polymer nanoscale films toward gamma irradiation," ACS Appl. Mater. Interfaces **7**, 19455 (2015).